Next generation 1.5 µm terahertz antennas: mesa-structuring of InGaAs/InAlAs photoconductive layers

H. Roehle*, R. J. B. Dietz, H. J. Hensel, J. Böttcher, H. Künzel, D. Stanze, M. Schell, and B. Sartorius

Fraunhofer Institute for Telecommunications, Heinrich-Hertz-Institut, Einsteinufer 37, 10587 Berlin, Germany
**roehle@hhi.fraunhofer.de*

Abstract: Mesa-structuring of InGaAs/InAlAs photoconductive layers is performed employing a chemical assisted ion beam etching (CAIBE) process. Terahertz photoconductive antennas for 1.5 µm operation are fabricated and evaluated in a time domain spectrometer. Order-of-magnitude improvements versus planar antennas are demonstrated in terms of emitter power, dark current and receiver sensitivity.

OCIS codes: (300.6495) Spectroscopy, terahertz; (260.5150) Photoconductivity.

References and links

1. M. Suzuki, and M. Tonouchi, "Fe-implanted InGaAs photoconductive terahertz detectors triggered by 1.56 µm femtosecond optical pulses," Appl. Phys. Lett. **86**(16), 163504 (2005).
2. N. Chimot, J. Mangeney, L. Joulaud, P. Crozat, H. Bernas, K. Blary, and J. F. Lampin, "Terahertz radiation from heavy-ion-irradiated In0.53Ga0.47As photoconductive antenna excited at 1.55 µm," Appl. Phys. Lett. **87**(19), 193510 (2005).
3. B. Sartorius, H. Roehle, H. Künzel, J. Böttcher, M. Schlak, D. Stanze, H. Venghaus, and M. Schell, "All-fiber terahertz time-domain spectrometer operating at 1.5 microm telecom wavelengths," Opt. Express **16**(13), 9565–9570 (2008).
4. E. R. Brown, "A photoconductive model for superior GaAs THz photomixers," Appl. Phys. Lett. **75**(6), 769 (1999).
5. L. Duvillaret, F. Garet, J.-F. Roux, and J.-L. Coutaz, "Analytical modeling and optimization of terahertz time-domain spectroscopy experiments, using photoswitches as antennas," IEEE J. Sel. Top. Quantum Electron. **7**(4), 615–623 (2001).

1. Introduction

Terahertz systems operated at 1.5 µm wavelength can benefit from the large variety of lasers and fiber components developed and matured originally for telecom applications. Thus compact, flexible and cost effective THz sensor systems can be assembled. For a long time, the photoconductive antennas (PCAs) for 1.5 µm had been the bottleneck. Low temperature (LT) growth of InGaAs on InP using molecular beam epitaxy (MBE) then gave the needed ultrafast response - similar to the case of LT GaAs. Unfortunately, in contrast to LT GaAs, LT InGaAs exhibits a high dark conductivity, so far preventing its use for PCAs. Hence alternative techniques like Fe-implantation [1] or ion-irradiation [2] of InGaAs have been tried - with limited success up to now. Recently a structure has been developed where thin (12 nm) InGaAs photoconductive layers are embedded between InAlAs trapping layers [3]. In this approach, the resistivity had been increased by several orders of magnitude. One hundred periods of LT InGaAs/InAlAs were grown in order to also achieve sufficient photo efficiency. THz antennas for 1.5 µm were fabricated, and good performance of a fiber coupled 1.5 µm time domain (TD) system was demonstrated [3]. In this paper we present developments on the next generation of 1.5 µm PCAs, especially by applying a kind of mesa-structuring of the photoconductive layers. The concept and its technological realization are described in parts 2 and 3. Electrical characteristics and THz output powers are subject of parts 4 and 5, respectively. Finally, in part 6 the improvements achieved in TD systems are evaluated.

#121674 - $15.00 USD Received 18 Dec 2009; revised 15 Jan 2010; accepted 15 Jan 2010; published 21 Jan 2010

2. Concept for improved PCA's by mesa structuring

A general disadvantage of photoconductive antennas with on-top metal contacts results from the decreasing in-plane electrical field component (Fig. 1) in the depth of the photoconductor [4]. In our multi-layer structure (100 periods InGaAs/InAlAs), unfortunately, this problem is enhanced due to the many interfaces at the intermediate InAlAs layers with higher bandgap. The interaction of photocarriers with the electric field is reduced, and in the receiver the carrier flow is hindered by the multi-layer design.

One possibility to solve this problem is to apply mesa-type structures with electrical side contacts (Fig. 1c). Here, the electrical field is directly applied even to deeper layers, and the current in the receiver does not need to traverse heterostructure barriers. The mesa structuring offers a second advantage: The photoconductive material can be removed, wherever it contributes to the dark current but not to the photo current (Fig. 1b). This because the photo-excited spot and thus the width of the photo-current region are in the 10 µm range. The dark current, however, flows between the full length (3 mm) of the antenna strip lines. Therefore, the area outside the optical excitation spot contributes about 300 times more to the dark current than the optically excited area itself. Since the semi-insulating (s.i.) InP substrate has a much higher resistivity than the photoconductive layers, the overall dark current can be significantly reduced by removing photoconductive material outside of the optically excited area or by structuring an isolating trench between electric contacts and those parts of the layer that do not contribute to photo-conductivity, as indicated in Fig. 1d and as visible in the SEM picture in Fig. 2b.

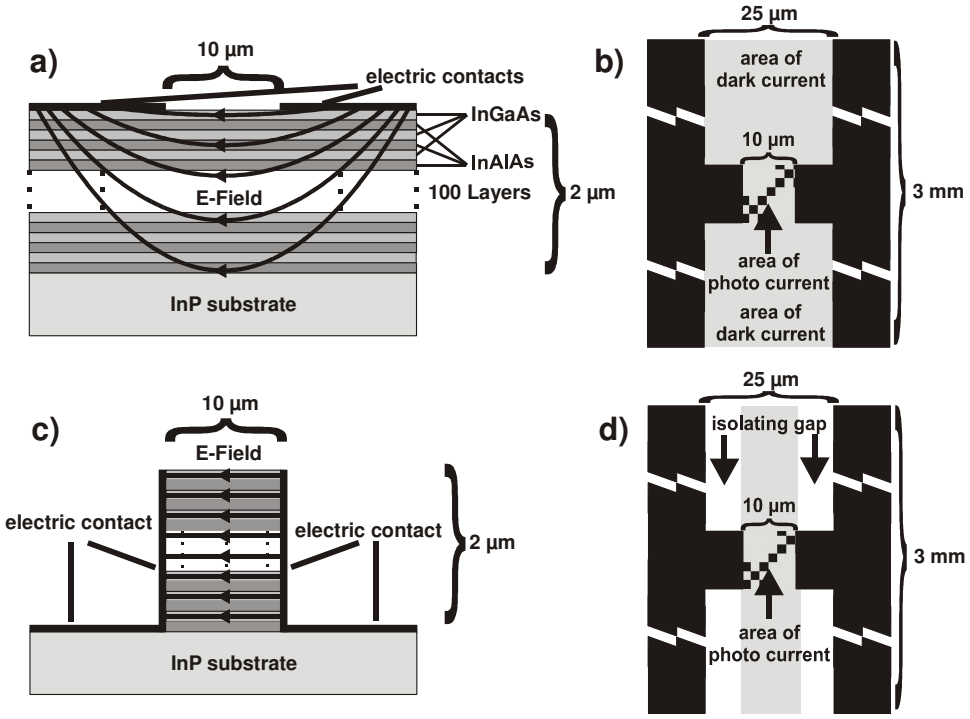

Fig. 1. Planar (a, b) versus mesa (c, d) structured antennas. Side view (a, c) and top view (b, d)

3. Mesa etching technique

The challenge in the mesa etching process is caused by the different materials in the multi-layer structure, the overall thickness, and the need for flat vertical walls for good electrical contact features. Key challenge is the extremely low etching rate of InAlAs. Wet chemical etching leads to strong undercuts of the InGaAs and thus has to be excluded. Even in an ion

#121674 - $15.00 USD Received 18 Dec 2009; revised 15 Jan 2010; accepted 15 Jan 2010; published 21 Jan 2010

beam etching (IBE) process, the InAlAs withstands the Ar^+ beam better than the photo mask, which consequently is removed before the process is ended. In addition, the etched flanks are rough and surface degradations come up during processing. So we employed a chemically assisted (Cl_2) ion beam etching process (CAIBE). The material is exposed to the Ar^+ beam and additionally to a stream of highly reactive Cl_2 gas. The etching of InAlAs is significantly accelerated, and by properly adjusting substrate temperature, the Ar^+ beam energy and intensity, and the flow rate of the Cl_2 gas stream, the etch rates for InGaAs and InAlAs can be balanced. After optimization, steep flanks with good surface quality have been achieved applying this process.

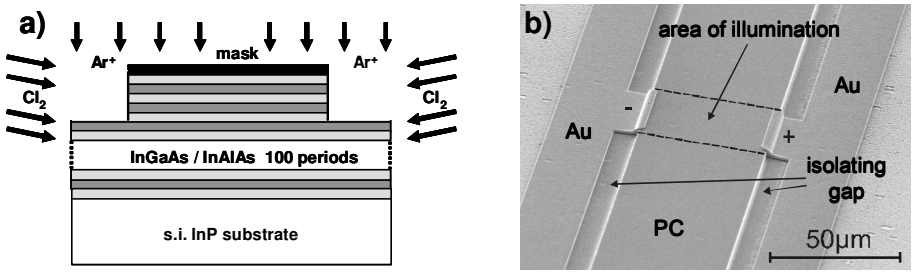

Fig. 2. (a) Scheme of the CAIBE Process, (b) SEM picture of a mesa-structured stripline antenna

The last step concerns the integration of the THz antennas with electric side contacts to the mesa structured photoconductor. Au is sputter-deposited and structured as shown in the SEM picture (Fig. 2b) for a strip line antenna. The metal side contact at the area of illumination can clearly be seen. In all other regions, isolating trenches separate metal and photoconductor, which go down to the s.i. InP substrate, and thus serve to minimize the dark current.

4. Electrical characteristics: mesa versus planar structures

First, the improvements of the photoconductive characteristics under CW illumination at 1.5 µm are investigated using dipole antennas with 10 µm gap and 25 µm strip line distance. For the previous planar structure (Fig. 3a) the photo current is only slightly increased relative to the (high) dark current. In Fig. 3b the improvements due to the mesa structure become clearly visible. The photo current at 10 mW optical power is now by a 5 times higher than the (low) dark current. The dark current is successfully reduced by removing the parasitic contributions from outside the excited photoconductive gap. This effect is studied in more detail in Fig. 3c comparing dark currents in planar and mesa structures. We measure a reduction of the dark current by a factor of 23. Although this is a notable reduction, just from geometry we would expect a significantly higher factor: The width ratio of exited spot to antenna strip lines is 10/3000, resulting in a factor 300. The width of the dipole gap is 10 µm while there are 25 µm between the antenna striplines, reducing the calculated geometrical improvement factor to 120. The measured improvement factor, however, is only 23. The origin of this discrepancy can be understood by looking at the photo currents as follows:

The effective photo currents - the differences between current with and without illumination - are depicted in Fig. 3d for planar and mesa structures. One can notice an increase of the photo current by a factor 5 for the mesa structured device. Excitation power and externally applied voltage are the same in both cases. Thus we attribute the improvement to the side contacts. The in-depth electrical field is higher for the mesa structures, and currents from the deeper layers go directly to the contacts, without crossing intermediate barriers of the heterostructure. This, however, also holds for the dark current through the mesa structure. Thus one can expect an increase similar to that for the photo current by a factor of 5. This explains the discrepancy observed for the dark current reduction discussed above.

#121674 - $15.00 USD Received 18 Dec 2009; revised 15 Jan 2010; accepted 15 Jan 2010; published 21 Jan 2010

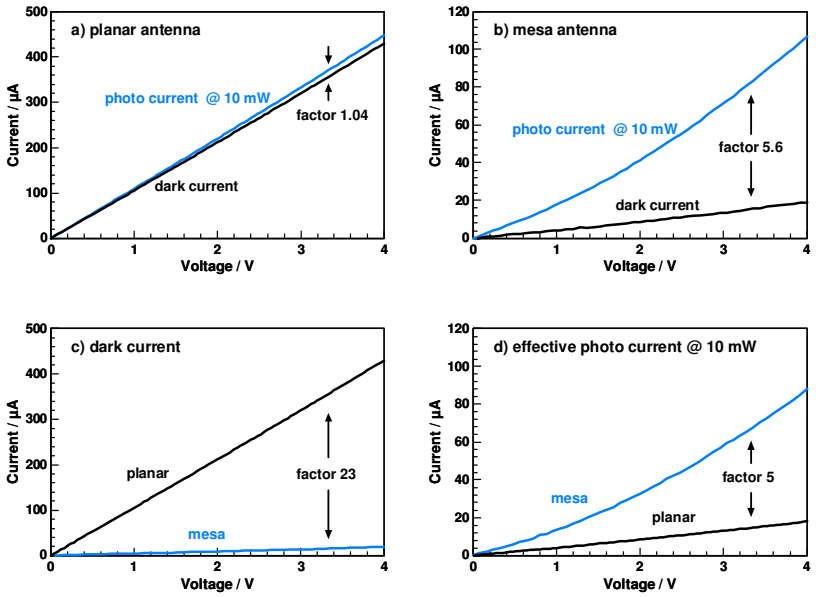

Fig. 3. Comparison of planar versus mesa antennas (dipole 25/10 µm): dark and photo current: (a) planar antenna (b) mesa antenna planar and mesa structure: (c) dark current (d) photo current at 10 mW minus dark current

In summary: Photo current, as well as dark current, in the photoconductive gap is increased by a factor 5 thanks to the side contacts of the mesa. Parasitic dark currents outside the gap are reduced by a factor 120 (dipole 25/10 µm, antenna length 3000 µm) thanks to removing the material contributing only to dark currents. The measured overall dark current is reduced by a factor 23 due to the coexistence of both effects.

5. Improving the THz output power

Next the improvement in THz output power with the mesa structure is studied. A factory calibrated Golay cell allows for absolute measurements of the averaged output power. The emitters are strip line antennas with a gap of 25 µm. The antennas are excited by 100 fs pulses at a center wavelength of 1.55 µm from a fiber ring laser (Menlo Systems) with a repetition rate of 100 MHz. The antennas of planar and mesa type are packaged into fiber coupled housings developed at HHI. An N_2 purged THz path with 2 inch parabolic mirrors focuses the emission onto the Golay cell. Optical excitation power and emitter bias voltage are varied within the measurements. Our results are summarized in Fig. 4. The THz output power at 40 mW mean optical excitation shows a quadratic behavior with increasing bias voltage, as expected within the scope of basic models [5]. The averaged THz power at 14 V and 40 mW is 0.33 µW, corresponding to a THz peak power of about 4.7 mW if a THz pulse width of 0.7 ps is assumed. With a bias of 25 V and 16 mW optical excitation power we measured an average THz output of 1.24 µW (17.7 mW peak) from the mesa antenna. In general, the increase in THz output power due to the mesa structuring is about a factor of 5 to 6.5, depending slightly on the optical excitation power and bias voltage.

The impact of the optical excitation power on THz emission (at 14 V bias voltage) is shown in Fig. 4b. Here the expected super-linear characteristics appear only at low excitation powers. A linear range follows, and for the mesa antenna even a sub-linear increase can be observed above 20 mW. We attribute this to saturation and/or screening effects, but further investigations are necessary to understand and to avoid these limitations. For the present devices an excitation power of 20 mW appears reasonable. In conclusion, mesa compared to planar antennas deliver five times higher THz output power at similar operating parameters.

#121674 - $15.00 USD Received 18 Dec 2009; revised 15 Jan 2010; accepted 15 Jan 2010; published 21 Jan 2010

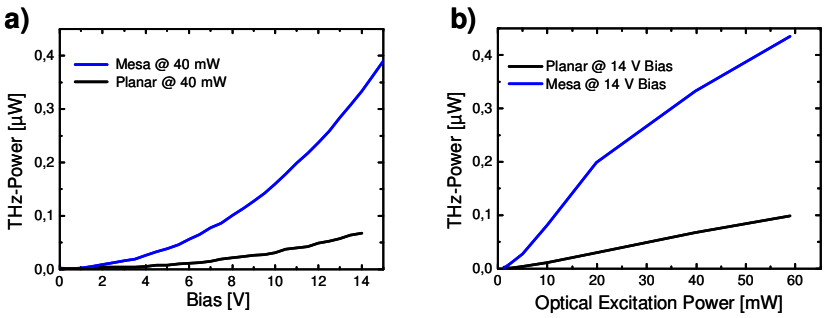

Fig. 4. THz output power measured with a Golay cell in dependence (a) on bias voltage, at 40 mW optical power, and (b) on optical power, at 14 V bias voltage

6. Performance of mesa antennas in a time domain system

The evaluation of the novel mesa-type PCAs is concluded by measurements in the time domain system shown in Fig. 5. Strip line (25 µm) emitters and dipole (10 µm) receivers are packaged into fiber coupled modules. The average excitation power is 20 mW for emitter and receiver respectively. The emitter bias voltage is 10 V, modulated at 5 kHz. The THz emission is focused by off-axis parabolic mirrors onto the detector, and the THz path is purged with dry nitrogen to avoid water vapor absorption (Fig. 5). The planar antennas are step by step replaced by the new mesa devices, first only on the emitter site, then only on the receiver site, and in the end at both sites. The difference between the minimum and the maximum values within one pulse of the received signal is taken as a measure for the performance of the respective configuration. The value obtained in the system with conventional planar antennas serves as a reference.

First, the emitter is changed from planar type to mesa type. The amplitude is increased by a factor 2.5 (Fig. 6). In order to compare this with the Golay cell results, where the THz power is measured, the pulse trace current values are squared and integrated. The improvement found here for the mesa in this example is a factor of 5.8 in power, which is in good agreement with the factor of 6.4 measured using the Golay cell for the underlying parameter values of 10 V and 20 mW. Next, we investigate planar emitters and mesa receivers (Fig. 6b). The amplitude is increased by a factor 11 - 12 compared to planar receivers. The mesa side contacts allow for an increased coupling of the THz field and a significantly improved charge transfer in the depth of the photoconductive layers since they allow current flow without traversing barriers and borders. As result, the improvements of mesa structures on the receiver are higher than on the emitter side.

Finally, we use mesa structures both for the emitter and the receiver. The measured improvement in amplitude is a factor of 27.5, corresponding to the product of the values for only emitter (x 2.5) or only receiver (x 11). The significant higher received signal allows the use of electronic preamplifiers with lower gain and thus higher bandwidth. So improved signal/noise ratio, higher speed of measurements and investigation of weaker signals are made possible by the novel antennas. In addition to the higher amplitude, we also observe that the THz pulse width is reduced by about 100 fs compared to the planar structure. Consequently, the Fourier spectrum (Fig. 6d) now extends beyond 4 THz, compared to 3 THz for the non-mesa antennas (not shown). Unfortunately, the relative noise floor of the FFT spectrum does not decrease proportionally with the increasing signal strength due to limitations in the absolute precision of the delay timebase.

#121674 - $15.00 USD Received 18 Dec 2009; revised 15 Jan 2010; accepted 15 Jan 2010; published 21 Jan 2010

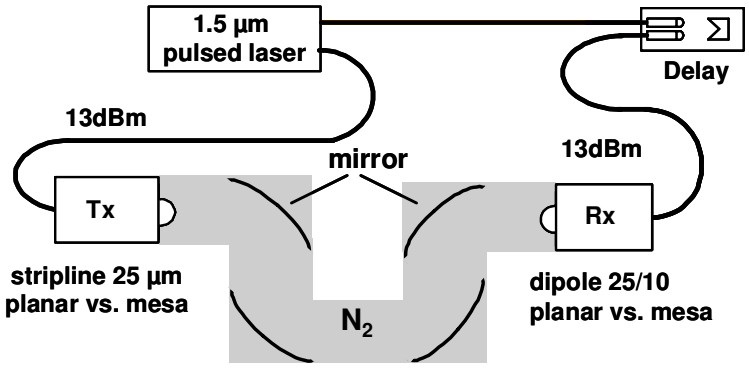

Fig. 5. Scheme of the THz Time Domain System

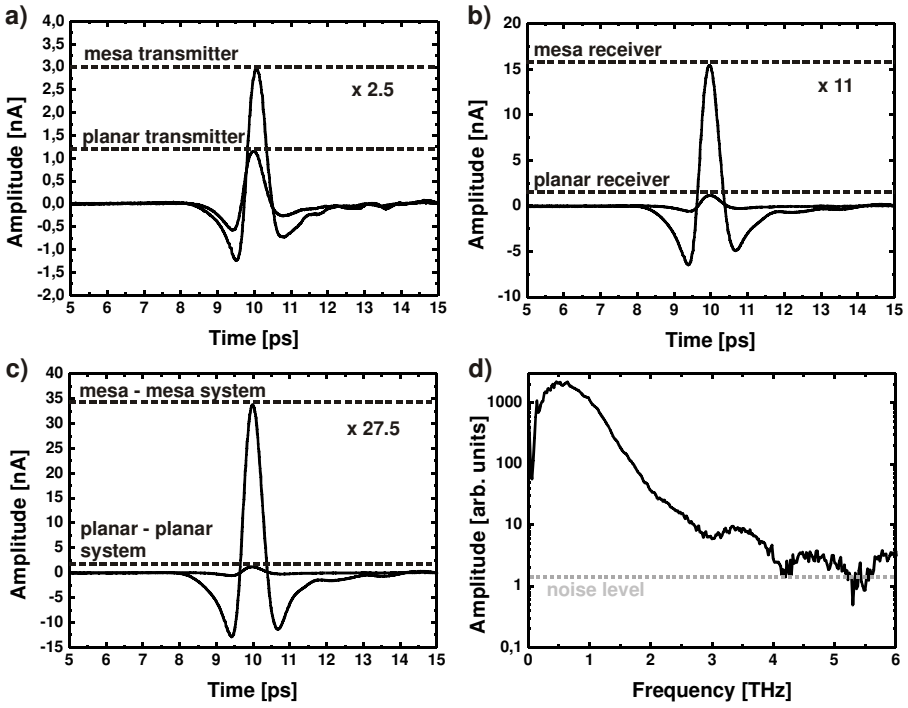

Fig. 6. Detected TD signal traces applying mesa antennas versus planar antennas: (a) mesa emitter, (b) mesa receiver, (c) mesa system, (d) FFT spectrum of mesa system

Summary and outlook

InGaAs/InAlAs photoconductive antennas for 1.5 µm operation have been improved by mesa-etching of the conductive layers. Electrical side contacts to the multi-layer structure are applied, and layers are removed in regions contributing only to parasitic dark currents.

Consequently, photo currents are increased by a factor 5 and parasitic dark currents are suppressed. The emitted THz power is increased by more then a factor 5 compared to conventional planar antennas, the receiver sensitivity is improved by a factor of 11. All in all, the complete mesa systems outperform the previous planar systems by a factor 27.5 in detected amplitude. The noise limit of the Fourier spectrum has been extended beyond 4 THz. Summarized, the new generation of THz antennas with mesa-structured photoconductive layers represents a considerable advancement for 1.5 µm THz TD systems.

#121674 - $15.00 USD Received 18 Dec 2009; revised 15 Jan 2010; accepted 15 Jan 2010; published 21 Jan 2010